

# Design, Manufacturing, and Numerical Simulation of a Tube-in-Tube High-Temperature Heat Exchanger with Microstructures to Enhance Heat Transfer

Andrea C. Hurtado Rivera<sup>a,\*</sup>, Frank B. Löffler<sup>b</sup>, Ethel C. Bucharsky<sup>b</sup>, Karl G. Schell<sup>b</sup>, Emma S. Thompson<sup>c</sup>, Nikolaus Nestle<sup>c</sup>, Hannah Schreyer<sup>c</sup>, Jan G. Korvink<sup>a</sup>, Jürgen J. Brandner<sup>a</sup>

<sup>a</sup>Institute of Microstructure Technology (IMT), Karlsruhe Institute of Technology, Eggenstein-Leopoldshafen, Germany

<sup>b</sup>Institute for Applied Materials – Ceramic Materials and Technologies (IAM-KWT), Karlsruhe Institute of Technology, Karlsruhe, Germany

<sup>c</sup>BASF SE, Ludwigshafen, Germany

[andrea.rivera@kit.edu](mailto:andrea.rivera@kit.edu)

The ever-increasing demands of the industry for higher power densities in heat transfer have led to the miniaturization of heat exchangers, which have been proven to provide an increased heat transfer capacity. Furthermore, the demand for increasing thermal efficiency, associated with high temperatures, calls for the implementation of high temperature-resistant materials. For this purpose, ceramics represent a good option as they can withstand high temperatures and corrosive environments whilst keeping good mechanical properties. In the present work, the design, simulation, and manufacturing of a novel ceramic tube-in-tube heat exchanger with integrated microstructures for the enhancement of heat transfer is presented. The fabrication was done by means of lithography-based ceramic manufacturing (LCM), a novel technique for additive manufacturing of ceramics.

## 1. Introduction

In the last decades, the miniaturization of devices and therefore process intensification has increased drastically in almost every area, from the semiconductor industry (Radamson, et al., 2019) and medicine technologies (Schumacher, et al., 2012) to process engineering (Charpentier, 2005). Heat exchangers profit greatly from miniaturization, as the power transferred increases with a decreasing distance between the heat source and sink, and with a decreasing characteristic length (Brandner, et al., 2006). Another way of increasing the power transferred is by inducing localized turbulences. This can be achieved by adding certain microstructures, such as microcolumns (Kandlikar, et al., 2013), or by increasing the surface roughness (Wu & Cheng, 2003).

The structuring of ceramics with micrometric accuracy poses a great challenge, and significant efforts have been made to address this. To manufacture micro heat exchangers, commonly, ceramic plates are mechanically machined in green state, stacked and afterwards sintered (Meschke, et al., 2005). Other approaches include low-pressure injection moulding (Alm, et al., 2008), laser machining (Mohammed, et al., 2018), and, most recently, a combination of additive manufacturing and laser machining (Hong, et al., 2019). Given that these methods are best applied to plates and/or simple planar geometries, their use for manufacturing complex 3D microstructures on the round profile of a tube proves limited. For complex cases, such as the one presented in this work, additive manufacturing might be the best-suited technique.

Recent improvements in additive manufacturing technologies allow for a greater flexibility in the realizable geometries and therefore, new possibilities for the optimization of heat exchangers. Currently, some of the most-used methods for additive manufacturing of ceramics are selective laser sintering (SLS) and lithography-based ceramic manufacturing (LCM). In SLS, parts are created layer by layer by fusing the needed area of a powder bed (with or without binders) with a laser beam. Travitzky et al. (2014) conducted an extensive review

of the advancements in SLS and other additive manufacturing techniques for ceramics. They concluded that the biggest disadvantage of SLS is the low relative density after sintering, spanning from 39% to 92% in most of the reviewed works, and 98% in only one of them.

In LCM, a slurry consisting of monomers, ceramic particles and photonitators is crosslinked by light stemming from Laser Emitting Diodes (LEDs) directed through a digital micro-mirror device (DMD); the process is described in detail by Schwentenwein et al. (2014). The green bodies must then undergo cleaning, debinding and sintering, to get rid of the polymer and to obtain a dense ceramic body, respectively. The relative density of technical ceramics (aluminium oxide, zirconium oxide, silicon nitride) achieved with LCM is above 98%, giving it an advantage over SLS (Lithoz GmbH, 2019).

In this work, the design, numerical simulation, and manufacturing of a tube-in-tube heat exchanger will be presented. The goal is for the heat exchanger to withstand high temperatures and high pressures, which allows it to be used as a reactor in process engineering. Another possible application, and the one for which this particular heat exchanger is being developed, is as a cell for high-temperature analysis by means of Nuclear Magnetic Resonance (NMR).

## 2. Design of the tube-in-tube heat exchanger

A cylindrical shape has been chosen to both enable high inner pressures and better utilize the space within the commercial gradient used in the NMR system, which has a cylindrical inner volume. The geometry of the heat exchanger consists therefore of two concentric ceramic cylinders. The heating medium will flow through the cavity between both cylinders. The inside of the inner cylinder shall act as the reaction chamber, where high pressures can be expected. A sketch can be seen in Figure 1a.

There are several approaches that can be used to determine the theoretical maximum pressure that the part can withstand. All the components of the system must be considered, such as connectors, but for the purpose of this paper, focus will be set solely on the ceramic cell. Several norms exist, such as the AD 2000 code of practice (Verband der Technischen Überwachungs-Vereine e.V., 2000), which regulate the design of pressure vessels and pipelines, and even include specifications for a brittle material, glass (AD2000-N4). However, these are only applicable for vessels with bigger dimensions and not appropriate for ceramic materials.

Another approach is given by Usbeck (2012), who formulated a dimensioning provision for ceramic parts, which takes into account the statistical nature of defects in ceramic materials. Due to dimensional constraints, the inner load-bearing wall has an inner diameter of 8 mm and outer diameter of 9.2 mm. The material selection process will be explained in Section 4 of this work, so for design purposes the three-point bending stress is known to be 395 MPa (Lithoz GmbH, 2019) and the Weibull modulus 11 (Schwentenwein & Homa, 2015). With this data, the maximum allowable stress of the inner wall according to Usbeck's approach is 190 MPa.

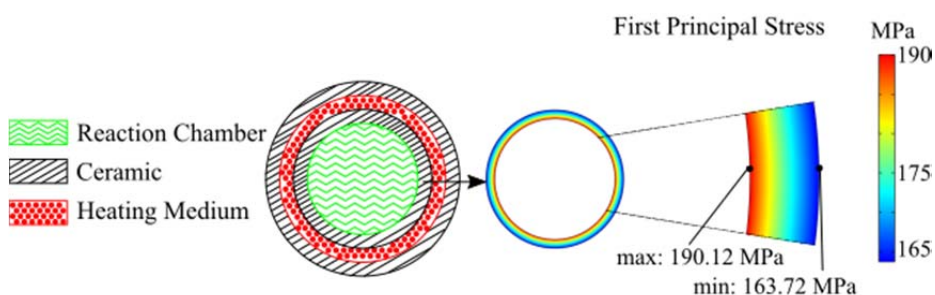


Figure 1. a) Sketch of heat exchanger. b) Simulation with inner pressure 26.4 MPa and wall thickness 0.6 mm

The relation between the inner pressure and the generated stress on the part can be determined by means of Barlow's formula or by running a solid mechanics simulation. In Figure 1b, the resulting first principal stress for the inner cylinder and an inner pressure of 26.4 MPa obtained with the Solid Mechanics Module of COMSOL Multiphysics 5.5 is shown. The inner pressure of 26.4 MPa gives a maximum first principal stress of 190 MPa. This means that the theoretical maximum inner pressure that the heat exchanger can withstand is 26.4 MPa. This theoretical result must still be validated with experimental data.

The design of the heat exchanger is arranged in a way that nitrogen can be used as heating medium, given that it is NMR-invisible and is suitable for high temperature applications. One of the highest heat transfer rates known to the authors can be achieved with the microstructures developed by Brighenti et al. (2013). With these, the flow was kept in a developing state and heat fluxes of 700 W/cm<sup>2</sup> with a relatively low pressure drop

were achieved. However, a compromise between the complexity of the geometry and fabrication accuracy in the micrometer range ( $<150\ \mu\text{m}$  within cavity) must be accomplished. In preliminary manufacturing tests, the microstructures proposed by Brighenti et al. could be fabricated as outer features. However, it was determined that it is not feasible to fabricate these microstructures within a cavity; the reasons for this will be explained in Section 4. Therefore, another geometry had to be chosen.

The best option from both manufacturability and heat transfer properties point of view is a staggered microcolumns array as investigated by (Brandner, et al., 2006). Brandner's experimental data shows that the staggered array has both a higher thermal power transferred for a given pump power and a higher heat transfer efficiency for a given mass flow rate than an aligned array and microchannels. These microstructures have also been extensively studied by other authors, such as Peles et al. (2005), who performed an analytical study of a staggered microcolumns configuration and validated it with experimental data, or Gerken (2020), who methodically compared experimental data of aligned, staggered, and staggered leaf-shaped microcolumns. The staggered microcolumns array was chosen for the presented heat exchanger. The outer appearance of the heat exchanger can be observed in Figure 2a, and the microcolumns array adapted to the round surface of the cylinder in Figure 2c.

For the heating medium, only two outlets and two inlets have been designed to facilitate the interfacing with the gas dosing system. Both outlets are on one end of the cylinder and both inlets are on the other end. At the outlets and inlets, a special shape has been designed for improving the flow distribution throughout the heat exchanger, it can be seen in Figure 2b.

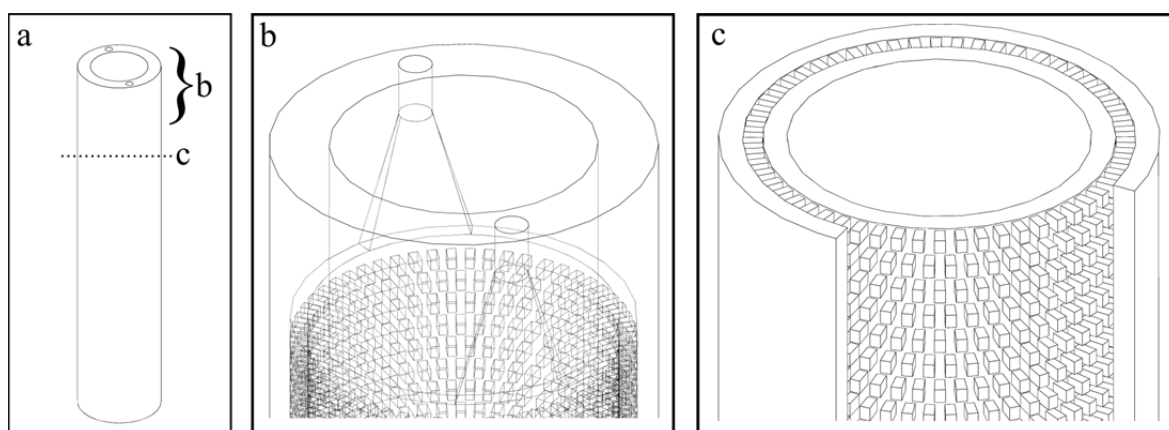


Figure 2. CAD Model of heat exchanger a) Outer appearance of heat exchanger (left). b) Flow distributor (middle). c) Staggered microcolumns array – lid and top cut for clarity – (right)

### 3. Computational Fluid Dynamics Simulation

For better understanding the fluid behaviour within the heat exchanger and further optimization of the process, computational fluid dynamics (CFD) simulations have been performed using the Heat Transfer Module of COMSOL Multiphysics 5.5, specifically Conjugate Heat Transfer. This module solves the fluid domains as non-isothermal and interfaces them with heat transfer within solids, taking into account the convection effects of the fluid. Using the maximum flow rate expected for the heating medium as a starting point for estimation, and due to the geometry, the turbulence model  $k-\omega$  is used, as it can better solve flows in near-wall regions (Kajishima & Taira, 2017). Due to the symmetry of the system, only 1/8 of the domain was modelled and the symmetry condition was used on the respective faces to reduce computational effort. The obtained results were then combined for postprocessing, as seen in Figura 3a. The outer surface was modelled as thermally insulated. Nitrogen and  $\text{Al}_2\text{O}_3$  were assigned as materials to both media and the solid part respectively. The heating medium and the medium within the reaction chamber are arranged in a counter-current configuration. As a first step, the medium within the reaction chamber has been modelled as pure nitrogen with expected flow rate up to 0.03 l/min. For a more accurate simulation of the system, the modelled material will be changed to match the properties of the chemicals that will be flowing through the inner cylinder. The optimization of the flow distributor, shown in Figure 2c, is within the scope of upcoming work, so for the purpose of these simulations, a homogeneous velocity distribution along the inlet will be assumed. As for the heating medium, a nitrogen flow rate of 16.4 l/min and an inlet temperature of  $500^\circ\text{C}$  were chosen as maximum values. The swirling of the flow downstream of each microcolumn could be observed, as shown in Figure 3b. These locally-induced turbulences account for the increase in heat transfer.

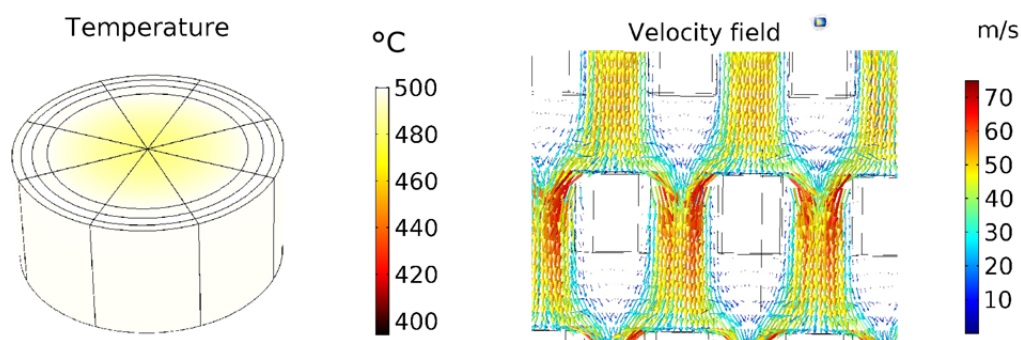


Figure 3. Results of CFD simulations of heat exchanger a) temperature (left) and b) enlargement showing swirls after microcolumns and velocity magnitude (right)

#### 4. Manufacturing

As previously stated, this heat exchanger is being developed for use in an NMR system. Therefore, it is of utmost importance to choose a material that is NMR-compatible and at the same time can withstand high temperatures. Some ceramics, such as yttrium-stabilized zirconium oxide ( $ZrO_2$ ) (Erlach, et al., 2010) and aluminium oxide ( $Al_2O_3$ ) (Arnold, et al., 2003), have already successfully been used for NMR cells. Both ceramics have good mechanical properties at high temperatures, hence fulfilling the requirements for the goal of this work. Ultimately,  $Al_2O_3$  was chosen, as its less demanding sintering parameters – lower sintering temperature and oxidizing environment – allow for a less specialized furnace.

Due to the complex geometry of the heat exchanger, the technique lithography-based ceramic manufacturing (LCM), developed by Lithoz GmbH, has been chosen. The printer used is the CeraFab 7500, which has a nominal resolution of 40  $\mu m$  and layer height between 25 and 100  $\mu m$  (Lithoz GmbH, 2020). To ensure a better dimensional accuracy, the smallest layer height, 25  $\mu m$ , was selected for the fabrication of the heat exchanger, with the downside of longer printing times. Lithoz GmbH offers two  $Al_2O_3$  slurries: LithaLox HP500 and LithaLox 350. One key difference between both of them is the dynamic viscosity (12 Pa\*s vs 8.5 Pa\*s at 20°C respectively), which makes LithaLox 350 more appropriate for the fabrication of small cavities. Hence, it was chosen for the manufacturing of the heat exchanger.

Although the chosen slurry has a relatively low dynamic viscosity, remnant material could still be found within the cavity after printing. To overcome this, a special cleaning routine had to be developed. The cleaning of the green bodies fabricated with LCM has already been identified as a critical step by other authors. Schwarzer et al. (2017) analyzed the influence of cleaning method, cleaning agent and waiting time for cleaning after printing on part quality. They concluded that the parts should be cleaned directly after printing, and that an ultrasonic bath should not be used, as it damages the green bodies by causing delamination. Scheithauer et al. (2018) gave important insight regarding the maximum time which the part can be exposed to cleaning agents. This time should be limited, as otherwise, the part swells and defects are introduced. The authors recommend not more than 5 minutes exposure.

Taking this into account, a cleaning routine for the heat exchanger was developed. The parts were cleaned directly after printing, and debound and sintered promptly afterwards. The cleaning fluid LithaSol 20, which is appropriate for use with LithaLox 350, and pressurized air were used for cleaning. The cleaning fluid was slowly pumped through one inlet, so as not to build “preferential paths” within the remnant slurry, which would complicate the cleaning of the rest of the cavity. This was followed by cleaning with pressurized air, to help the cleaning fluid go through the part. This process was repeated several times. A list with debinding and sintering parameters for medium parts (1mm < wall thickness < 3mm), and specially determined for LithaLox 350, was received from Lithoz GmbH. The debinding and sintering programs had a maximum temperature of 1100°C and 1650°C respectively. The sintered heat exchanger is shown in Figure 4a.

It is important to note that a support structure was used during sintering of the part, to prevent stress-induced crack formation. After sintering, the parts were analysed by means of X-Ray Microtomography (Micro-CT) in order to observe the inner cavity and look for possible cracks without destroying the part. As previously explained, one of the biggest challenges is the cleaning of the cavity to free it from remnant slurry. This becomes even more challenging for high aspect ratios, which is the case of this cavity, with a length of 60 mm and a gap of 0.6 mm before sintering. The aforementioned cleaning routine proved successful, as the inner microstructures are completely free of remnant slurry, which can be seen in Figure 4b.

No cracks could be found either, which can be partly attributed to the support structure used, which allows for a stress-free shrinkage of the heat exchanger during debinding and sintering. Using the microCT picture, the dimensions of the microcolumns and walls after sintering were measured. The inner wall has a thickness of 0.6 mm, the microcolumns have an average width of 0.25 mm and height of 0.35 mm, and the gap size between both cylinders is 0.45 mm.

It is important to note that this heat exchanger could be achieved due to a compromise between dimensions of the green body, simplicity of geometry and an adequate cleaning routine, as well as heat transfer capabilities and high pressure resistance. Initial manufacturing tests using the microstructures from Brighenti et al. (2013) within the cavity proved non-feasible, due to overpolymerization resulting from scattering light and due to the difficulty of cleaning such a complex inner geometry.

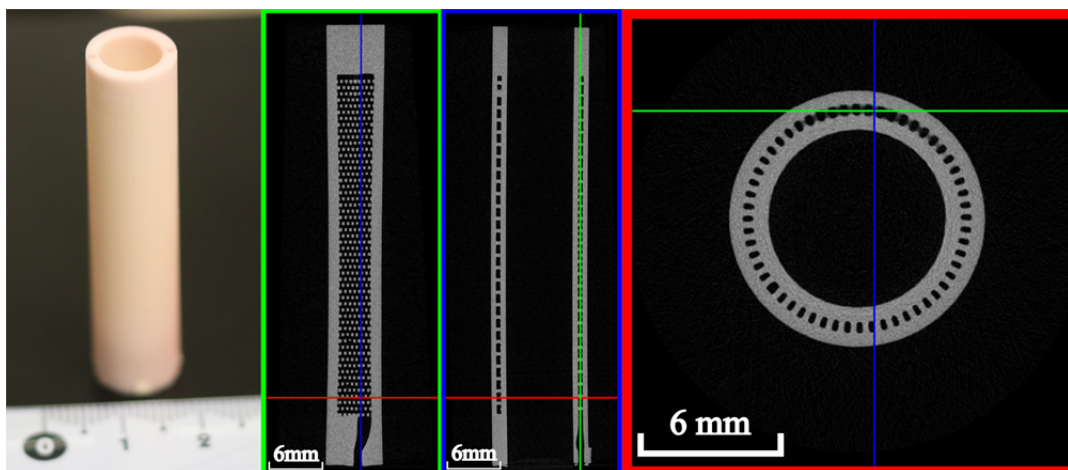


Figure 4. a) Picture of heat exchanger after sintering (left). b) MicroCT scan of heat exchanger -scanned at 70 kV, 141  $\mu$ A- (middle to right).

## 5. Conclusions

The improvements and breakthroughs in additive manufacturing techniques, especially in the field of ceramics, enable the fabrication of parts and devices with great geometrical complexities that could not have been done before. Using lithography-based ceramic manufacturing, a tube-in-tube heat exchanger with microstructures for enhanced heat transfer has been fabricated. Special attention was paid to the cleaning process of the green body, as the remnant slurry must be removed from the cavity before sintering. The microcolumns follow a staggered array pattern. Each microcolumn has a width of 250  $\mu$ m and a height of 350  $\mu$ m, and the cavity between both cylinders in which they are has a gap size of 450  $\mu$ m. The whole heat exchanger has a length of 50 mm. A part fabricated using LCM, with a cavity with such an aspect ratio, is not known to the authors from literature.

Further development and analysis of the tube-in-tube heat exchanger is currently being conducted. The aim is to develop a longer part, up to 15 cm in length. The fluid behaviour and thus thermal performance of the heat exchanger will continue to be optimized using CFD simulations. A test bench is currently being built, in which both the thermal properties and mechanical stability of the heat exchanger will be tested. In this test bench, the mass flow rate of both fluids as well as the inlet temperature of the heating medium can be set and measured. The temperature and pressure of both fluids before and after the heat exchanger can also be measured. This experimental data will be used to validate the numerical simulations.

## References

- Alm, B., Imke, U., Knitter, R., Schygulla, U., & Zimmermann, S. (2008). Testing and simulation of ceramic micro heat exchangers. *Chemical Engineering Journal*, 135, 179-184.
- Arnold, M. R., Kalbitzer, H. R., & Kremer, W. (2003). High-sensitivity sapphire cells for high pressure NMR spectroscopy on proteins. *Journal of Magnetic Resonance*, 161(2), 127–131.
- Brandner, J. J., Anurjew, E., Bohn, L., Hansjosten, E., Henning, T., Schygulla, U., . . . Schubert, K. (2006). Concepts and realization of microstructure heat exchangers for enhanced heat transfer. *Experimental Thermal and Fluid Science*, 30(8), 801-809.

- Brighenti, F., Kamaruzaman, N., & Brandner, J. J. (2013). Investigation of self-similar heat sinks for liquid cooled electronics. *Applied Thermal Engineering*, 59(1-2), 725-732.
- Charpentier, J.-C. (2005). Process Intensification by Miniaturization. *Chemical Engineering & Technology*, 28(3), 255-258.
- Erlach, M. B., Munte, C. E., Kremer, W., Hartl, R., Rochelt, D., Niesner, D., & Kalbitzer, H. R. (2010). Ceramic cells for high pressure NMR spectroscopy of proteins. *Journal of Magnetic Resonance*, 204(2), 196-199.
- Gerken, I. (2020). Efficiency improvement of miniaturized heat exchangers. Karlsruhe: Karlsruher Institut fuer Technologie (KIT).
- Hong, Y., Lei, J., Heim, M., Song, Y., Yuan, L., Mu, S., . . . Peng, F. (2019). Fabricating ceramics with embedded microchannels using an integrated additive manufacturing and laser machining method. *Journal of the American Ceramic Society*, 102(3), 1071-1082.
- Kajishima, T., & Taira, K. (2017). *Computational Fluid Dynamics: Incompressible Turbulent Flows*. Cham: Springer International Publishing.
- Kandlikar, S. G., Colin, S., Peles, Y., Garimella, S., Pease, R. F., Brandner, J. J., & Tuckerman, D. B. (2013). Heat Transfer in Microchannels - 2012 Status and Research Needs. *Journal of Heat Transfer*, 135(9), 091001.
- Lithoz GmbH. (2019). *Lithoz: Produkte: Materialien*. Retrieved November 24, 2020, from <https://www.lithoz.com/produkte/material>
- Lithoz GmbH. (2020). *Lithoz: Produkte: 3D Drucker*. Retrieved September 17, 2020, from [www.lithoz.com/produkte/3D-drucker](http://www.lithoz.com/produkte/3D-drucker)
- Meschke, F., Riebler, G., Hessel, V., Schürer, J., & Baier, T. (2005). Hermetic Gas-tight Ceramic Microreactors. *Chemical Engineering & Technology*, 28(4), 465-473.
- Mohammed, M. K., Umer, U., Rehman, A. U., Al-Ahmari, A. M., & El-Tamimi, A. M. (2018). Microchannels Fabrication in Alumina Ceramic Using Direct Nd:YAG Laser Writing. *Micromachines*, 9(8).
- Peles, Y., Kosar, A., Mishra, C., Kuo, C.-J., & Schneider, B. (2005). Forced convective heat transfer across a pin fin micro heat sink. *International Journal of Heat and Mass Transfer*, 48(17), 3615-3627.
- Radamson, H. H., He, X., Zhang, Q., Liu, J., Cui, H., Xiang, J., . . . Wang, G. (2019). Miniaturization of CMOS. *Micromachines*, 10(5).
- Scheithauer, U., Schwarzer, E., Moritz, T., & Michaelis, A. (2018). Additive Manufacturing of Ceramic Heat Exchanger: Opportunities and Limits of the Lithography-Based Ceramic Manufacturing (LCM). *Journal of Materials Engineering and Performance*, 27(1), 14-20.
- Schumacher, S., Sartorius, D., Ehrentreich-Förster, E., & Bier, F. F. (2012). Miniaturization for Point-of-Care Analysis: Platform Technology for Almost Every Biomedical Assay. *EJIFCC*, 23(3), 70-75.
- Schwarzer, E., Götz, M., Markova, D., Stafford, D., Scheithauer, U., & Moritz, T. (2017). Lithography-based ceramic manufacturing (LCM) – Viscosity and cleaning as two quality influencing steps in the process chain of printing green parts. *Journal of the European Ceramic Society*, 37(16), 5329-5338.
- Schwentenwein, M., & Homa, J. (2015). Additive Manufacturing of Dense Alumina Ceramics. *International Journal of Applied Ceramic Technology*, 12(1), 1-7.
- Schwentenwein, M., Schneider, P., & Homa, J. (2014). Lithography-based Ceramic Manufacturing: A Novel Technique for Additive Manufacturing of High-Performance Ceramics. *AST (Advances in Science and Technology)*, 60-64.
- Travitzky, N., Bonet, A., Dermeik, B., Fey, T., Filbert-Demut, I., Schlier, L., . . . Greil, P. (2014). Additive Manufacturing of Ceramic-Based Materials. *Advanced Engineering Materials*, 16(6), 729-754.
- Usbeck, A. K. (2012). Auslegung von keramischen Strukturbauteilen unter mehraxialer statischer und zyklischer Beanspruchung. Hamburg.
- Verband der Technischen Überwachungs-Vereine e.V. (2000). AD 2000-Merkblatt. Berlin: Beuth.
- Wu, H., & Cheng, P. (2003). An experimental study of convective heat transfer in silicon microchannels with different surface conditions. *International Journal of Heat and Mass Transfer*, 46(14), 2547-2556.